Tuijin Jishu/Journal of Propulsion Technology
ISSN: 1001-4055
Vol. 44 No. 5 (2023)

Activating Illite kaolinite clay with CTAB for adsorbing Methylene blue: Isotherms, Kinetics, and thermodynamics studies

Sara Bahemmi [1], Ammar Zobeidi[1,2,*], Salem Atia[1], Salah Neghmouche Nacer [2], Djamel Ghernaout [3,4] Noureddine Elboughdiri [3,5].

[1] Pollution and waste treatment laboratory (PWTL), University of Ouargla, P.O. Box 511, 30000, Algeria.
[2] Department of Chemistry, Faculty of Exact Sciences, University of El-Oued, P.O. Box 789, El-Oued 39000.
[3] Chemical Engineering Department, College of Engineering, University of Ha'il, P.O. Box 2440, Ha'il 81441, Saudi Arabia.
[4] Chemical Engineering Department, Faculty of Engineering, University of Blida, Blida 09000, Algeria.
[5] Chemical Engineering Process Department, National School of Engineers Gabes, University of Gabes, Gabes 6029, Tunisia.

*Corresponding author: zobeidi.aa@gmail.com

Abstract

In this study, a stable multilayered adduct of maghemite surfactant and clay was created by sandwich-like electrostatic self-assembly of cationic polyelectrolytes of cetyltrimethylammonium bromide (CTAB) with illite kaolinite (IKaol) clay. The adsorptive property of IKaol/CTAB towards MB from . Aquatic system uptake was investigated. Its characteristics were analysed using X-ray powder diffraction, Fourier transform-infrared spectroscopy, scanning electron microscopy, energy dispersive X-ray spectroscopy, and the zero point of charge. To attain higher performance of the IKaol/CTAB for MB adsorption, the primary key factors that influence the MB dye, such as (A: loading CTAB into the composite matrix of IKaol), adsorbent dose (B: 0.02–0.06 g), pH (C: 4–10), temperature (D: 30–60 °C), and time (E: 5–60 min) , were optimised using the Box–Behnken design method. The obtained results show that the highest MB removal efficiency of 86.24 % was observed at the following significant interactions: AB, BC, and AC and at optimum adsorption operation parameters (A: 0%, B: 0.06 g, C: 7, D: 45◦C, and E: 17.5 min). At these optimum conditions, the best adsorption capacity of MB dye (114.94 mg/g) was recorded at 45°C. The most effective isotherms and kinetic models were the Freundlich and pseudo-second-order kinetic models. The MB dye adsorption mechanism by IKaol can be assigned to several interactions, such as electrostatic attractions, *n-π* interaction, and hydrogen bonding interactions. The results of this study demonstrate the viability of IKaol as a promising precursor for the creation of an efficient adsorbent that can be used to remove cationic dye from an aqueous environment.

1. Introduction

Since a lot of wastewater containing dye is released from human activities without being treated, there has been a substantial decline in the quality of the environment and drinking water worldwide, even at low concentrations [1-3]. Dyes in effluents are exceedingly dangerous to humans and harm the aquatic biological system [4, 5]. Biological treatments [5, 6], photochemical degradation [7], chemical precipitation [8, 9], membrane separation [10, 11], and adsorption are some of the technologies currently being developed for removing dyes [12, 13]. Methylene blue (MB) and other organic cationic dyes are considered to be more hazardous to humans and other living things than anionic dyes [14, 15]. This severe environmental issue can be solved by lowering or eliminating

the dye content of wastewater before its release into the aquatic environment [16].
The adsorption method, which has been widely employed for treating dye wastewater pollution, has the benefits of high efficiency, simplicity of design and availability, and non-generation of harmful compounds [17, 18]. However, the effectiveness of any adsorption procedure depends on the selection of a suitable medium [19]. Moreover, several researchers have focussed heavily on the study of adsorption technology employing inexpensive adsorbents [20]. Natural clays have garnered much attention as adsorbents because of their distinct capacity to remove contaminants from water at low concentrations and their reduced production cost [21]. Illite kaolinite (IKaol), which is found in rocks worldwide and has a crystalline structure, is a well-known, abundant, and affordable natural clay [22, 23]. IKaol is often composed primarily of illite and kaolinite, along with other minerals such as quartz and mica [8]. Depending on the pH of the solution, the surface of IKaol has a continuous structurally negative charge due to the isomorphous substitution of Si^{4+} by Al^{3+} in the silica layer [24], which is an active adsorption site for the removal of colours from wastewater [25]. IKaol has recently been used in a few studies as an adsorbent for removing water pollutants such as dyes [26] and heavy metal ions [27]. However, the direct application of pure IKaol clay is ineffective in efficiently removing anionic dyes, such as MB, from aqueous solutions. Therefore, it is advantageous to chemically modify pure IKaol with a suitable chemical agent to achieve a more favourable surface charge, which will enhance the clay's adsorption capacity [28-30]. One approach to modify the surface of IKaol is to use organic substances such as cetyltrimethylammonium bromide (CTAB) [31]. When ion exchange occurs in IKaol and organoclay is formed, the surface charge, hydrophobicity, and physicochemical properties of the surfaces change.
This study thoroughly evaluated the adsorption performance of MB using IKaol modified with CTAB from aqueous solutions. For multivariate modelling and optimising MB adsorption onto IKaol/CTAB considering input variables (loading CTAB into IKaol) in addition to adsorption essential parameters, response surface methodology (adsorbent dose, solution pH, temperature, and contact time) was used. In-depth research was also conducted on the adsorption kinetics, isotherms, and thermodynamics of MB dye removal using IKaol/CTAB.

2. Materials and methods

2.1. Reagents and materials

Raw illite kaolin (IKaol) clay was collected from El Oued in southern Algeria. The dye used in the study was MB (chemical formula: $C_{16}H_{18}N_3ClS$, λ_{max} = 664 nm, pK_a: 3.5, and MW: 319.86 g/mol) purchased from Sigma-Aldrich. Chemical products, such as CTAB (chemical formula: $C_{19}H_{42}BrN$, and MW: 364.46 g/mol), hydrogen peroxide (H_2O_2), acetic acid (80%), sodium hydroxide (NaOH), silver nitrate ($AgNO_3$), sodium carbonate (Na_2CO_3), sodium acetate ($C_2H_3NaO_2$), and hydrochloric acid (HCl), were purchased from Merck (Germany). All chemicals and reagents used in this study were of analytical grade and did not require additional purification.

2.2. Preparation of the IKaol/CTAB composites

The clay was purified to remove all crystalline phases and organic matter according to a method reported in the literature [15, 23, 32] to obtain 2 µm particles. Initially, 150 mL of a buffer solution of pH 4.8 (16 g sodium acetate and 10 mL of acetic acid) was placed in a beaker, and 10 g of IKaol clay was slowly added under constant stirring. The Ikaol clay was treated with 50 mL of 6% H_2O_2 to remove organic impurities. The resulting solution was transferred to a graduated tube and allowed to decant for ~8 h. Subsequently, the float layer is collected at a depth of 10 cm to produce particles smaller than 2 µm. The clay was recovered by vacuum filtration, washed with distilled water, and dried in an oven at 105 °C for 24 h. After drying, the Ikaol clay was crushed to a particle size of 100 mesh.

To fulfil the Box–Behnken design (BBD) optimisation process, a series of modified IKaol/CTAB composites were prepared as organic– nano clay by exchanging interlayer cations with CTAB in ratios with IKaol before dissolving in 80 mL HCl (4.10^{-4} M) under vigorous stirring at 80 °C for 3 h and leaving overnight. The residue was sonicated (30 min) to remove unreacted CTAB. The organic– nanoclay was washed perfectly until it

became free from Cl^-, confirmed by $AgNO_3$ testing. The preparation mentioned above was repeated to produce IKaol/CTAB-25 (75% IKaol: 25% CTAB) and IKaol/CTAB-50 (50% IKaol:50% CTAB). The composite powder was sieved to a constant particle size of 150 < particles size < 250 μm for future use. The entire scheme of the IKaol/CTAB composite material preparation is shown in Figure 1.

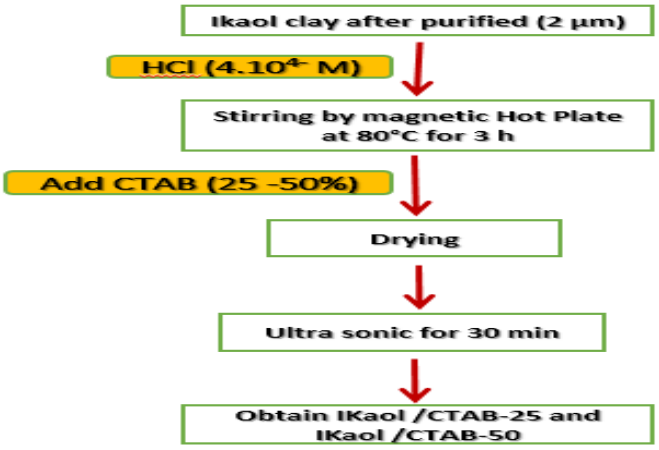

Figure 1. Schematic synthesis steps of IKaol/CTAB.

2.3. Sample characterization

To understand the amorphous and crystalline character of the produced materials, the X-ray diffraction (XRD) patterns were obtained using the XRD model PAN analytical X Pert Pro PMD with CuK = 1.5406 Å at wide-angle range (2Θ value 5° - 80°), running at 40 kV and 30 mAof IKaol, IKaol/CTAB-50, and IKaol/CTAB-25. The Fourier transform infra-red (FTIR) spectrophotometer model Schimadzu 8202PC was used to characterise the functional groups of IKaol before and after MB dye adsorption. The Hitachi TM3030Plus Tabletop Microscope from Tokyo (Japan) was used for scanning electron microscopy (SEM) and energy-dispersive X-ray (EDX) analysis to identify the morphological features and surface characteristics of IKaol before and after exposure to MB dye. This allowed direct verification of the purity, presence, and distribution of particular elements in the solid sample. A method previously described by Babic et al. [33] was used to determine the zero point of charge (pH_{pzc}) of IKaol

2.4. Design of experiments

The effects of five parameters, including loading of CTAB into IKaol (A), adsorbent dosage (B), solution pH (C), temperature (D), and time (E) on the adsorption of MB dye onto the surface of the IKaol composite were optimized and studied in this work using BBD. The levels of the used independent parameters and their coded values are shown in Table 1. Preliminary tests were used to define the range of these independent characteristics. The experimental results were analyzed, and the MB dye clearance was predicted using Eq. (1):

$$Y = \beta_0 + \sum_{i=1}^{k} \beta_i \chi_i + \sum_{i=1}^{k} \beta_{ii} \chi_i^2 + \sum_{i=1}^{k} \sum_{j=1}^{k} \beta_{ij} \chi_i \chi_j + \varepsilon \quad (1)$$

where: Y is an objective to optimize the response, x_i and x_j represent the response of MB dye removal, k indicates the number of variables, i and j denote the index numbers for variables, β_0 is the constant coefficient, β_i is the linear coefficient, β_{ii} is the quadratic coefficient, β_{ij} is the interaction coefficient, and ε represents a random error.

Table 1. Experimental levels of independent factors and their codes in Box–Behnken design (BBD).

Codes	Variables	Level 1(-1)	Level 2 (0)	Level 3 (+1)
A	Loading (%)	0	25	50
B	Adsorbent dose (g)	0.02	0.04	0.06
C	pH	4	7	10
D	Temperature (°C)	30	45	60
E	Time (min)	5	17.5	30

Optimization and investigation of the effects of the five input parameters (i.e., A: loading (0-50%), B: adsorbent dose (0.02-0.06 g), C: solution pH (4-10), D: temperature (30 - 60 °C), and E: time (5-30 min)) on MB dye removal R (%) using IKaol composites were carried out using 46 experiments (runs) following BBD. Table 2 displays the BBD matrix and the MB dye removal response results (%). A specific amount of adsorbent was added to a 250 mL Erlenmeyer flask with 100 mL of MB dye solution inside. A UV-vis spectrophotometer with a maximum wavelength of 664 nm (HACH DR 3900) was used to measure the MB dye concentration. Eq. (2) was used to express R (%) as follows:

$$R(\%) = \frac{C_0 - C_e}{C_0} \times 100 \quad (1)$$

where, C_0 and C_e represent the initial and equilibrium concentrations of MB dye (mg/L), respectively.

2.6. Batch adsorption studies

The best MB dye removal (86.24%) was found in experiment 4 (Table 2, under the following experimental conditions: loading (A:0%, indicating that IKaol), adsorbent dosage (B) 0.06 g in 50 mL), pH (C) 7, temperature (D) 45°C, and contact time (E) 17.5 min. As a result, the batch adsorption inquiry used these ideal experimental parameters. Using the same methodology, batch adsorption studies for MB adsorption were performed with different starting MB concentrations (50-300 mg/L) and contact periods from 0 to 140 min. Using Eq. (3), the equilibrium adsorption capacity (q_e) of MB was determined as follows:

$$q_e = \frac{(C_0 - C_e)V}{W} \quad (3)$$

where: V is the volume of the MB dye solution (L) and W is the total amount of the adsorbent (g).

Table 2 . Five parameters for the Box–Behnken design (BBD) matrix and experimental data regarding MB dye removal using IKaol/CTAB.

Run	A: CTAB loading (%)	B: Absorbent dose (g)	C: pH	D: Temperature (°C)	E: Time (min)	MB removal (%)
1	25	0.04	7	30	30	29.19
2	0	0.04	7	60	17.5	76.16
3	50	0.04	10	45	17.5	42.33
4	0	0.06	7	45	17.5	86.24
5	0	0.04	7	45	30	81.05
6	25	0.04	7	45	17.5	45.01
7	25	0.04	7	60	30	35.33
8	25	0.04	7	45	17.5	45.01
9	25	0.06	7	45	30	53.29
10	50	0.04	7	45	30	42.02
11	25	0.04	4	30	17.5	25.5
12	25	0.04	7	60	5	18.96

13	50	0.04	7	45	5	29.997
14	50	0.02	7	45	17.5	21.92
15	25	0.02	7	60	17.5	15.04
16	25	0.02	4	45	17.5	15.3
17	50	0.04	4	45	17.5	34.02
18	25	0.04	7	45	17.5	45.01
19	50	0.04	7	30	17.5	36.96
20	25	0.02	7	45	30	24.349
21	25	0.04	10	45	30	41.3
22	25	0.04	10	60	17.5	42.04
23	0	0.04	7	45	5	64.739
24	25	0.04	10	45	5	36.16
25	25	0.04	7	30	5	14.666
26	25	0.04	7	45	17.5	45.01
27	25	0.02	10	45	17.5	25.78
28	0	0.04	7	30	17.5	58.39
29	25	0.04	7	45	17.5	45.01
30	25	0.06	7	30	17.5	37.975
31	25	0.06	10	45	17.5	51.36
32	25	0.06	7	60	17.5	39.989
33	50	0.04	7	60	17.5	30.75
34	0	0.04	10	45	17.5	79.95
35	25	0.02	7	30	17.5	2.82
36	25	0.04	4	45	5	25.09
37	25	0.04	4	45	30	38.02
38	0	0.02	7	45	17.5	60.54
39	25	0.02	7	45	5	9.01
40	50	0.06	7	45	17.5	53.03
41	0	0.04	4	45	17.5	72.15
42	25	0.06	7	45	5	43.25
43	25	0.04	10	30	17.5	26.7
44	25	0.04	7	45	17.5	45.01
45	25	0.06	4	45	17.5	44.3
46	25	0.04	4	60	17.5	26.635

3. Results and discussion

3.1. Characterization

XRD analysis assessed the amorphous and crystalline nature of the prepared materials. The XRD patterns of (a) IKaol and (b) IKaol/CTAB are shown in Fig. 2. It can be seen that IKaol (Fig. 2a) has a strong diffraction peak at a diffraction angle (2θ) of 26.1°, as well as less intense peaks at 2θ of 19.7°, 20.3°, 24.8°, 35.1°, and 39.1°. All are linked to kaolinite. Illite diffraction peaks were discovered at 2θ of 29.1° and 42.4°. Quartz was found at 2θ of 20.9 and 26.6° [15, 23]. As depicted in Fig. 2b, the introduction of a surfactant expands the basal spacing within the resulting organoclay. This expansion signifies the presence of CTA^+ ions between the clay layers, which reduces the amount of hydrated water. It is well established that the quantity of surfactant added directly influences the degree of interlayer expansion in IKaol [34]. Decreases in the 2θ values of IKaol were at 26.1°. 29.1°. In addition, new diffraction peaks appeared at 2θ = 14.3°, 20.8°, and 42.7° in the IKaol/CTAB sample, indicating an

arrangement of CTAB interlayer clay galleries. This provides evidence that CTAB intercalation occurs in clay intersheets.

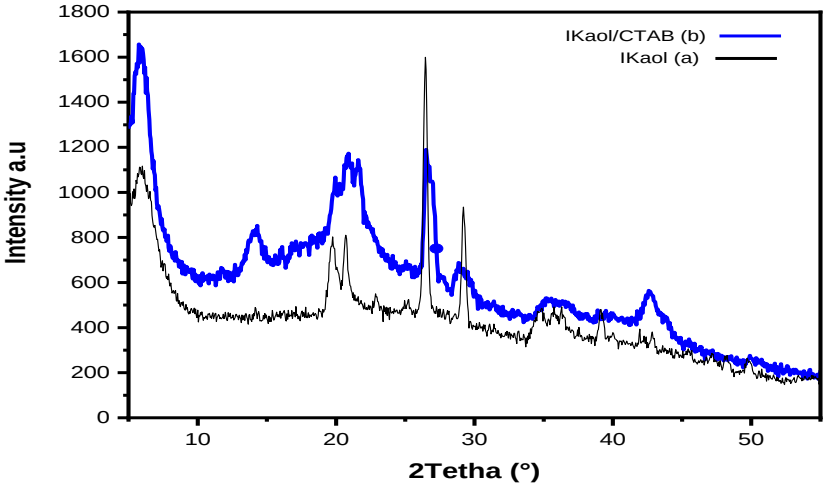

Figure 2. X-ray diffraction (XRD) pattern of (a) IKaol, (b) IKaol/CTAB.

The FTIR spectrum of IKaol (Fig. 3a) exhibits prominent peaks between 3695 and 3420 cm^{-1}, which can be correlated with the stretching vibrations of the O– H bonds. A distinctive peak at 1633 cm^{-1} corresponds to the bending vibration of coordinated water molecules [32, 35]. Furthermore, the characteristic peaks at 914 and 420 cm^{-1} are assignable to the stretching vibrations of Si–O– Si bonds in both kaolinite and illite. Meanwhile, the peak at 3620 cm^{-1} could be associated with the deformation of -OH groups connected to Al [15]. The FTIR spectrum of IKaol after the adsorption of the MB dye (Fig. 3b) displays the same bands in the spectrum of IKaol with slight shifting of some bands, indicating that the functional groups of IKaol were involved in the MB dye adsorption. Furthermore, a new band between 1200 and 1400 cm^{-1} can be attribute to the aromatic rings (C=C) of the MB dye adsorbed on the surface of IKaol [36].

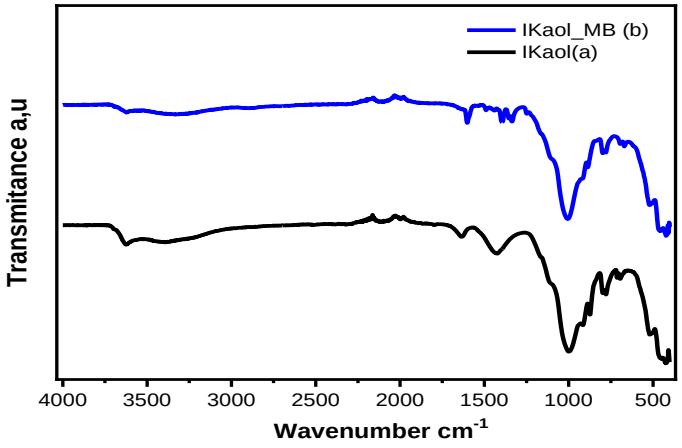

Figure 3. FTIR spectra of (a) IKoal and (b) IKoal after MB dye adsorption.

Moreover, SEM-EDX analysis was performed to identify the surface morphology and chemical composition. Figure 4 displays the SEM images and EDX spectra of (a) IKaol and (b) after MB dye adsorption. As shown in

Fig. 4a, the surface morphology of IKaol is irregular and heterogonous with crevices. The EDX spectrum of IKaol contains elements C, O, Al, Si, Fe, K, Na, and Mg. These elements are present in kaolinite, illite, and other clay constituents. Furthermore, the surface structure of the IKaol composite material following MB adsorption (Fig. 4b) appeared to be more compact because of the loading of the MB dye molecules onto its surface. The spike in the carbonation rate in the related EDX spectrum indicates that the MB dye is on the surface of IKaol.

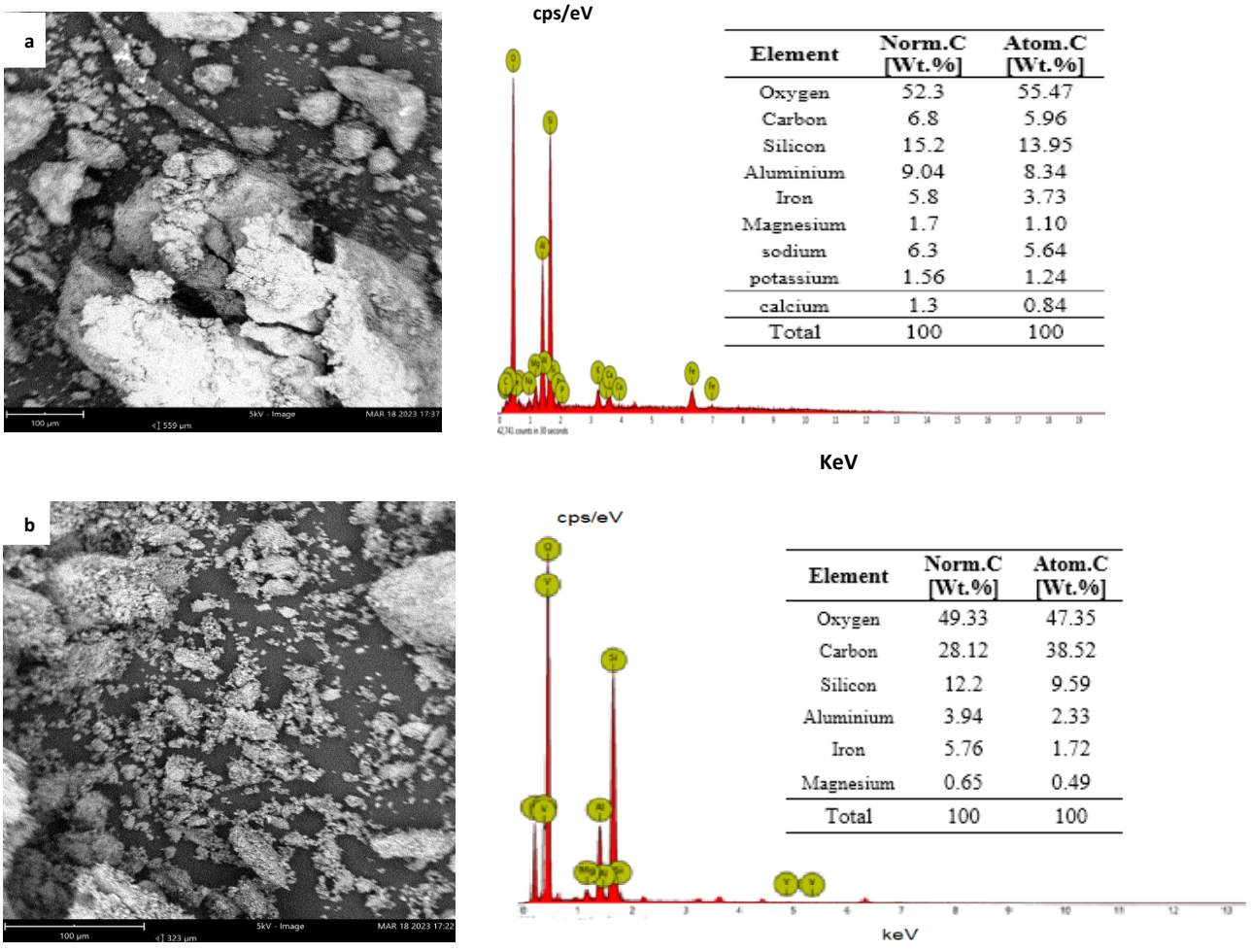

Element	Norm.C [Wt.%]	Atom.C [Wt.%]
Oxygen	52.3	55.47
Carbon	6.8	5.96
Silicon	15.2	13.95
Aluminium	9.04	8.34
Iron	5.8	3.73
Magnesium	1.7	1.10
sodium	6.3	5.64
potassium	1.56	1.24
calcium	1.3	0.84
Total	100	100

Element	Norm.C [Wt.%]	Atom.C [Wt.%]
Oxygen	49.33	47.35
Carbon	28.12	38.52
Silicon	12.2	9.59
Aluminium	3.94	2.33
Iron	5.76	1.72
Magnesium	0.65	0.49
Total	100	100

Figure. 4. SEM images and EDX spectra of (a) IKoal and (b) IKoal after the adsorption of the MB dye.

3.2. Parametric optimisation of Box–Behnken design (BBD)

Using BBD, we determined whether the adsorption input parameters of loading (A), adsorbent dosage (B), solution pH (C), temperature (D), and contact time (E) had independent or combined effects on MB dye removal. As shown in Table 3, a statistical analysis of the experimental results for MB dye removal was confirmed by analysis of variance (ANOVA). The *F*-value and *p*-value for the BBD model are 215.01 and <0.0001, respectively (Table 3). These findings [34] demonstrate the statistical importance of the BBD model for MB dye removal. The coefficient of determination (R^2) was 0.99, indicating a strong correlation between the measured and expected levels of MB dye removal. The BBD model's components are statistically significant when the p-value is less than 0.05 (Prob > *F* 0.0500) under the given conditions. As a result, the terms A, B, C, D, E, AD, BD, CD, A2, B2, C2, D2, and E2 presented in the BBD design are statistically significant regarding the removal of MB. Terms with *p*-values

greater than 0.05 are excluded from the quadratic polynomial equation to obtain the best fit of the BBD model. The quadratic polynomial equation in Eq. (4) describes the relationship between the investigated parameters and the response (MB dye removal).

$$\text{MB removal (\%)} = +45.01 - 18.01A + 14.66B + 4.03C + 3.29D + 6.41E - 5.99AD - 2.55BD + 3.55CD + 16.84A^2 - 6.99B^2 - 3.45C^2 - 12.58D^2 - 6.80E^2 \quad (4)$$

Table 3. Analysis of variance (ANOVA) of the MB dye removal response surface quadratic model (Df: degree of freedom).

Source	Sum of Squares	Df	Mean Square	F-value	p-value
Model	16311.78	20	815.59	215.01	< 0.0001
A-Loading	5190.91	1	5190.91	1368.49	< 0.0001
B-Dose	3442.02	1	3442.02	907.43	< 0.0001
C-pH	260.86	1	260.86	68.77	< 0.0001
D-Temper	173.60	1	173.60	45.77	< 0.0001
E-Time	658.91	1	658.91	173.71	< 0.0001
AB	7.32	1	7.32	1.93	0.1771
AC	0.0650	1	0.0650	0.0171	0.8969
AD	143.76	1	143.76	37.90	< 0.0001
AE	4.60	1	4.60	1.21	0.2815
BC	2.92	1	2.92	0.7709	0.3883
BD	26.04	1	26.04	6.87	0.0147
BE	7.02	1	7.02	1.85	0.1858
CD	50.45	1	50.45	13.30	0.0012
CE	15.17	1	15.17	4.00	0.0565
DE	0.8519	1	0.8519	0.2246	0.6397
A^2	2475.69	1	2475.69	652.67	< 0.0001
B^2	427.05	1	427.05	112.58	< 0.0001
C^2	104.38	1	104.38	27.52	< 0.0001
D^2	1382.43	1	1382.43	364.45	< 0.0001
E^2	404.68	1	404.68	106.69	< 0.0001
Residual	94.83	25	3.79		
Cor Total	16406.61	45			

The normal probability of the externally studentized residuals is shown in Fig. 5a. This figure depicts whether the distribution of residuals is normal. Points on a normal distribution should essentially lie in a straight line. Because the points in Fig. 5a are in a straight line, it can be assumed that their distribution is normal [15]. The normal distributions of the residuals demonstrate that the assumptions were reasonable and independent [37]. Fig. 5b

displays the correlation between the actual and expected MB dye clearance values. Based on Fig. 5b, the expected and actual positions were typically close. Hence, the experimental outcomes were deemed acceptable. Finally, Fig. 5c plots the residuals and the run number. The fact that all data were obtained in the residual rings (3 in Fig. 5c) indicated that the model was viable and could be used to establish the optimal working conditions that provide the highest removal of the MB dye [38].

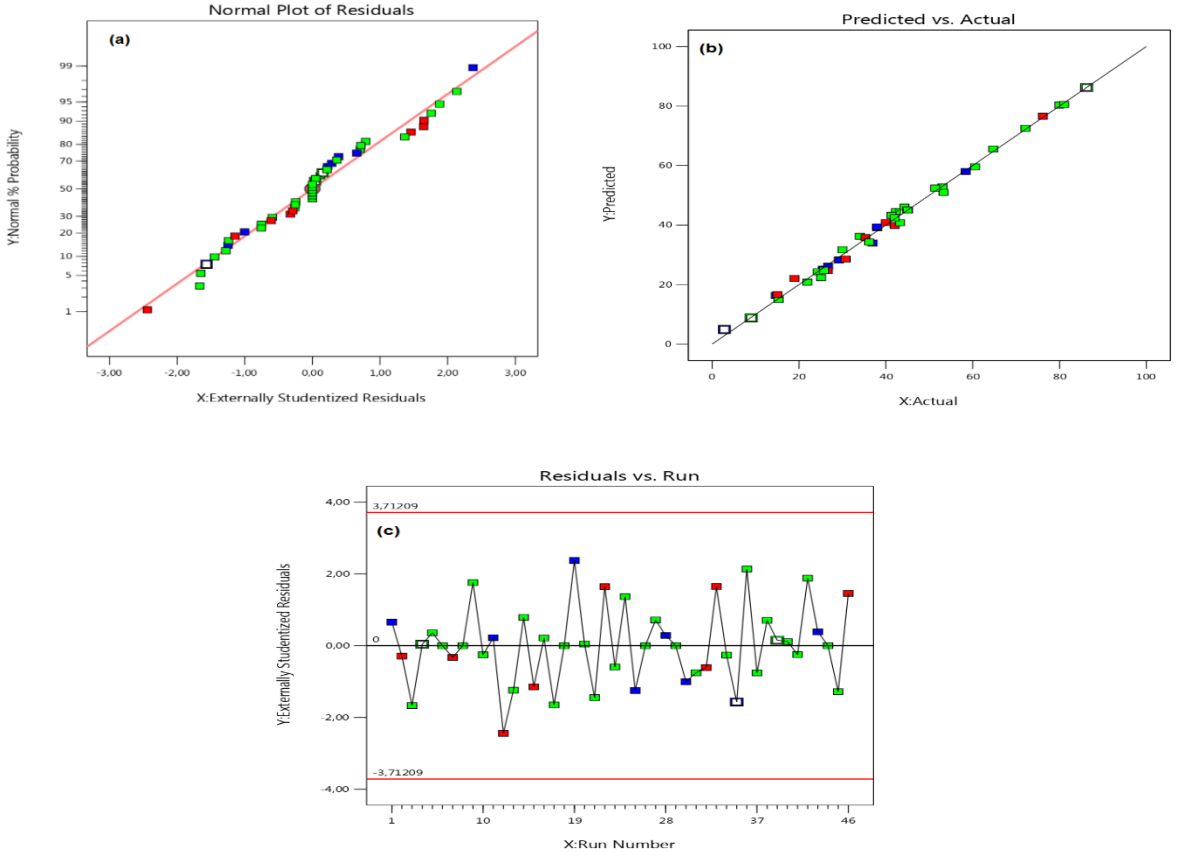

Figure 5. Plots of (a) the normal (%) probability of residuals, (b) actual values vs. predicted values, and (c) residuals vs. the run order.

3.3. Significant Interactions in the Adsorption Process

Investigated was the significant impact of the interaction between the two input parameters on MB dye removal. Statistics show that the interaction between temperature (D) and loading (A) has an impact on the elimination of MB dye (*p*-value <0.0001). The remaining variables, such as the 0.06 g adsorbent dosage and pH 7 of the solution, do not change during this time. Fig. 6a shows a 3D response surface plot of the effect of the interaction between loading and temperature on MB dye removal, showing that the removal of the dye increased as the loading of the IKaol/CTAB matrix decreased (from 0 to 50%). Additionally, the IKaol material may reach the ideal alignment between surface area and amine group content, achieving the best adsorptive performance. Further, as shown in Fig. 6a, the removal of the MB dye somewhat increased as the temperature was lowered to 30°C. This finding indicates that the adsorption of MB dye molecules onto the surface of IKaol may have an exothermic nature.

By holding the other operation parameters (CTAB loading 0%, pH of 7, and time of 17.5 min) constant, a further significant interaction of solution dose (B) with temperature (D) was the last statistically substantial interaction for the elimination of MB (p = 0.0146. The effect of the interaction between the adsorbent dose and time on MB dye removal (%) is shown in a 3D response surface plot in Fig. 6b. This Figure depicts that the MB dye removal

increased with an increase in adsorbent dose from 0.02 to 0.06 g; this result can be attributed to the increase in the adsorbent's active sites. Additionally, Fig. 6b demonstrates how dropping the temperature from 60 to 30°C improved the elimination of MB dye. This result shows the exothermic character of the MB adsorption process by the IKaol surface, which will be covered in more detail in the section below

Finally, there is a statistically significant (p-value = 0.0012) interaction between solution pH (C) and temperature (D) on MB dye elimination. The other factors (0% CTAB loading, 0.06 g of adsorbent, and 17.5 min) are constant. Fig. 6c depicts a 3D response surface showing the relationship between temperature and solution pH. The plot demonstrates that as the pH of the solution dropped from 10 to 4, the amount of MB dye removed (%) increased from 2.82 to 86.24. Furthermore, as can be seen in Fig. 6d, the pH_{pzc} of the IKaol is found to be 7.5. The IKaol can typically acquire negative surface charges at pH levels over pH_{pzc}, which results in a significant electrostatic attraction between the IKaol and MB dye cations, as given in Eq. (5):

$$IKaol - SiO^- + MB^+ \longleftrightarrow IKaol - SiO^- - {}^+MB \quad (5)$$

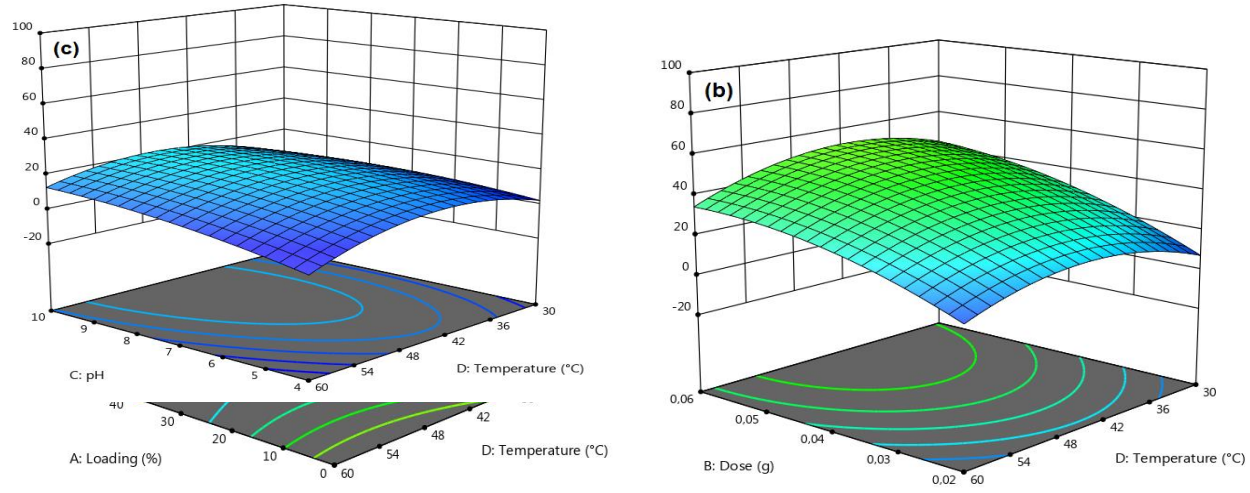

Figure 6. (a) 3D plot of the synergistic interaction of loading and the solution temperature on the MB removal; (b) 3D plot of the solution dose and the solution temperature; (c) 3D plot of the pH and solution temperature; (d) pH_{pzc} of IKaol.

3.4. Adsorption Study

We investigated the impact of contact duration on the adsorption of MB dye at various starting MB dye concentrations (50 to 300 mg/L) onto the surface of IKaol. The study's other variables, including the adsorbent dosage (0.06 g/100 mL), solution pH (7), and temperature (45°C), were held constant. The graphs of the IKaol q_t adsorption capacity (mg/g) against time (min) at various initial MB dye starting concentrations are displayed in Fig. 7. The adsorption capacity of IKaol toward MB dye molecules rose from 35.95 to 178.49 mg/g when the concentration of MB dye was increased from 50 to 300 mg/L (Fig. 7). This outcome could be explained by the driving force created by a large concentration gradient affecting the transport of the MB dye molecules to the interior pores and active sites in IKaol [39].

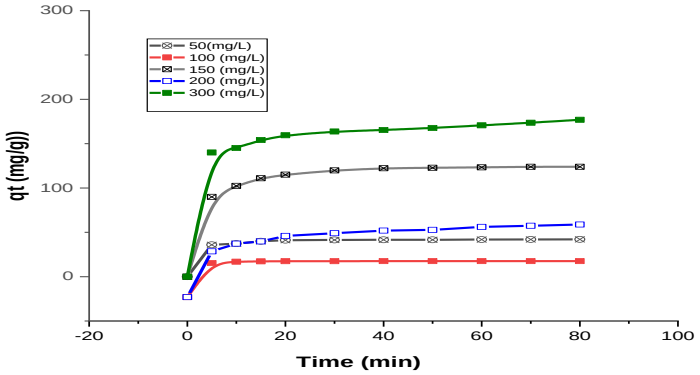

Figure 7. Effect of the initial MB concentration on the IKaol adsorption capacity as a function of the contact time (dosage 0.06 g, pH 7, temperature 45°C, agitation speed = 150 strokes/min, and volume of solution = 100 mL).

3.5. Adsorption kinetics

Adsorption kinetic is a vital character to understand the adsorption behavior of MB on the IKaol surface and inspect the adsorption mechanism. In this regard, pseudo-first-order (PFO) and pseudo-second-order (PSO) kinetic models were applied. The equations of the kinetic models PFO [40] and PSO [41] are presented in a non-linear form in Eqs. 6 and 7, respectively, as follows:

$$q_t = q_e\,(1 - exp^{-k_1 t}) \quad (6)$$

$$q_t = \frac{q_e^2\, k_2 t}{1 + q_e k_2 t} \quad (7)$$

where: q_t (mg/g) is the amount of MB dye adsorbed at time t (min), k_1 (1/min) is the rate constant of PFO, and k_2 (g/mg×min) is the rate constant of PSO.

Table 4 contains the kinetic models' parameters. The experimental findings (Table 4) lead to the conclusion that the PSO model describes the adsorption of MB dye molecules by the IKaol adsorbent because of the better correlation coefficient (R^2) values and the excellent fit between the estimated and experimental q_e (i.e., $q_{e,exp}$) values than it was in the case of the PFO kinetic model. This finding suggests that the chemisorption phenomenon predominates in the adsorption of MB dye molecules on the IKaol surface [41].

Table 4. PFO and PSO kinetic parameters for MB adsorption by IKaol

Concentration (mg/L)	$q_{e.exp}$ (mg/g)	PFO			PSO		
		$q_{e.cal}$ (mg/g)	k_1 (1/min)	R^2	q_{ecal} (mg/g)	k_2*10^2 (g/mg×min)	R^2
50	33.8	31.15	0.0023	0.66	32.15	8.873	1
100	75.5	74.39	0.05018	0.90	75.76	7.26	1
150	104.7	101.86	0.0899	0.956	104.38	0.499	0.99
200	107.6	104.37	0.0495	0.96	108.70	0.191	0.99
300	113.7	112.86	0.0899	0.95	113.28	0.107	0.99

3.6. Adsorption isotherm

Adsorption isotherm is significant in describing the interaction between MB dye molecules and IKaol. The most commonly utilized isotherms, namely Langmuir [42], Freundlich [43], and Temkin [44], are adopted for analyzing the equilibrium adsorption data and calculating the adsorption capacity of IKaol. The non-linear forms of the Langmuir, Freundlich, and Temkin are expressed in Eqs. (8) - (10), respectively, as follows:

$$\frac{C_e}{q_e} = \frac{q_{max}\, K_a\, C_e}{1 + K_a\, C_e} \quad (8)$$

$$q_e = K_F\, C_e^{\frac{1}{n}} \quad (9)$$

$$q_e = \frac{RT}{b_T} (\ln K_T C_e) \quad (10)$$

where: C_e (mg/L) is the concentration of MB dye at equilibrium, q_{max} (mg/g) is the maximum quantity of the MB dye per unit mass of IKaol, q_e (mg/g) is the amount of MB dye uptake at per unit weight of Kaol, K_a (L/mg) is Langmuir constant, K_F (mg/g)(L/mg)$^{1/n}$ is the Freundlich constant, n is the dimensionless constant that indicates the adsorption intensity, K_T (L/mg) is Temkin constant, T (K) is temperature, R (8.314 J/mol×K) is the universal gas constant, and b_T (J/mol) represent adsorption intensity and heat of adsorption, respectively.

Table 5. Isotherm model parameters for the MB adsorption by the IKaol composite material at 45°C.

Adsorption isotherm	Parameter	Value
Langmuir	q_{max} (mg/g)	114.94
	K_a (L/mg)	1.3385
	R^2	0.99
Freundlich	K_F (mg/g) (L/mg)$^{1/n}$	52.01
	n	3.73
	R^2	0.82
Temkin	K_T (L/mg)	27.82
	b_T (J/mol)	149.75
	R^2	0.782

According to Table 5, the uptake of MB dye by IKaol obeys the Langmuir isotherm model, which is better than the Freundlich and Temkin adsorption isotherm models due to its higher coefficient of determination (R^2 = 0.99) value compared to the other models. This finding suggests that the adsorption occurred on the homogenous surfaces through the monolayer coverage [45]. Moreover, the q_{max} for the IKaol was found to be 114.94 mg/g at 45°C based on the Langmuir model. Thus, the q_{max} of MB dye onto IKaol was compared with other adsorbents reported in the literature for removing MB, as listed in Table 6, revealing that IKaol represents a promising and efficient adsorbent for the removal of a cationic dye (MB) dye from an aqueous environment.

Table 6. Adsorption capabilities of various adsorbents.

Adsorbents	q_{max}(mg/g)	References
Alginate–organobentonite beads (1/1 w/w)	972.29	[1]
Dragon fruit skin	640	[2]
Brazilian montmorillonite	300.3	[3]
Fe_3O_4-CTMAC/SEIA-Mt	246	[4]

Iraqi red kaolin	240.4	[5]
Magnetic chitosan/clay beads	82	[6]
Egyptian ferruginous kaolinite	59.3	[7]
Algerian kaolin	52.76	[8]
Cellulose/clay composite-I	37.8	[9]
HCl activated Nteje Clay	24.04	[10]
Moroccan Illitic	13.6	[11]
IKaol	114.94	This study

3.7. Adsorption thermodynamics

Adsorption thermodynamic parameters are executed to study the adsorption process of MB dye onto the IKaol surface in terms of feasibility and spontaneity, in addition to estimating the degree of randomness at the interface of MB dye with the IKaol surface. Adsorption thermodynamic parameters, including Gibbs free energy change ΔG◦(kJ/mol), entropy change (ΔS˚) (kJ/molK), and enthalpy change ΔH˚ (kJ/mol) were obtained using Eqs. (11) - (13) [32, 38]:

$$\Delta G° = -RTLn\ K_d \quad (11)$$

$$K_d = \frac{q_e}{C_e} \quad (12)$$

$$LnK_d = \frac{\Delta S}{R} - \frac{\Delta H°}{RT°} \quad (13)$$

The values of thermodynamic parameters (ΔH˚ and ΔS˚) were calculated by plotting lnK_d against 1/T (Figure 8), where slope and intercept represent ΔH˚ and ΔS˚, respectively.

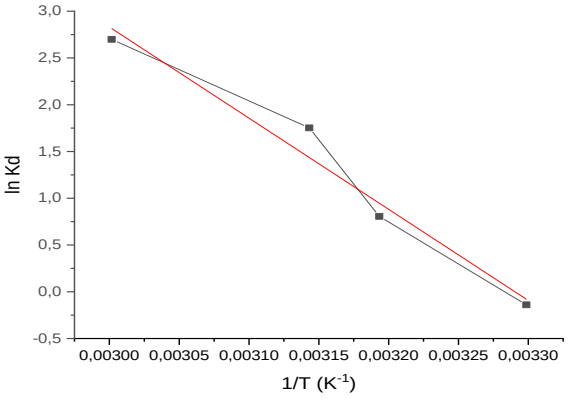

Figure 8. Van't Hoff plot for MB adsorption onto IKaol (dosage 0.06 g, pH 7, temperature 45 °C, agitation speed = 150 strokes/min, and volume of solution = 100 mL).

According to the obtained results in Table 7, the ΔG˚ with negative values demonstrate that the adsorption process of MB dye onto the IKaol was a spontaneous and favorable reaction [55]. Moreover, the enthalpy values for MB were estimated with negative signs, indicating that the adsorption process of MB by IKaol is exothermic. This observation aligns with the BBD parametric optimization results presented in Figure 8. The entropy values were also estimated with positive signs, suggesting the increased randomness at the solid–solution interface during the adsorption of MB onto IKaol [56], and this could be caused by the interaction between the dye and the spots on the material where it can stick.

Table 7. Thermodynamic characteristics for the MB adsorption on the IKaol composite material.

T (K)	lnk_d	ΔG° (kJ/mol)	ΔH° (kJ/mol)	ΔS° (kJ/molK)
303.15	6.259	-15.78	-4.69	0.051
313.15	6.584	-22.20		
323.15	8.529	-17.68		
333.15	8.629	-23.89		

3.8. Adsorption mechanism

The surface of IKaol contains adsorption sites like silanol (≡SiOH), aluminol (≡AlOH) groups, and mineral edge hydroxyl (-OH) groups [57, 58]. Concerning IKaol's pHpzc, the surface gains a negative charge in alkaline conditions due to hydroxyl group deprotonation [59]. Taking into account this, the adsorption mechanism of MB dye onto the IKaol surface involves multiple interactions, as illustrated in Figure 9. Significant is the electrostatic attraction that significantly binds MB dye to IKaol. This underscores the crucial role of electrostatic forces, specifically between positively charged MB dye cations and negatively charged sites on IKaol's surface.

Additionally, the adsorption mechanism also encompasses H-bonding interactions between hydrogen atoms present on the IKaol surface and N atoms within the structure of the MB dye. Finally, the *n-π* interaction arises from the dispersion of lone pair electrons of O atoms into the *π* orbitals of the aromatic rings in the dye's structure. In light of the details above, it can be inferred that these interactions had a crucial contribution in improving the adsorption phenomenon of the IKaol adsorbent to the MB dye.

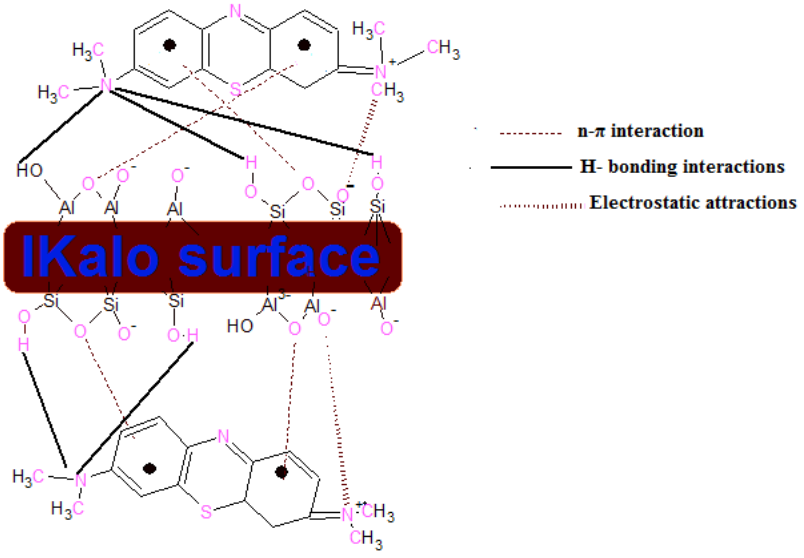

Figure 9. MB dye adsorption mechanism on the IKaol surface.

4. Conclusion

In this work, a unique IKaol was successfully applied to remove MB dye from an aqueous environment, and the study optimized key factors influencing the process. These factors included loading CTAB into the IKaol matrix, adsorbent dose, solution pH, contact time, and temperature. The Box-Behnken design method was employed to determine the optimal adsorption parameters by examining the impacts of five independent components. The best MB removal rate (98.76%) was achieved with optimal working conditions: loading CTAB: 0%, adsorbent dose: 0.06 g, pH seven, temperature 45°C, time 17.5 min. At these optimized conditions, the adsorption capacity of MB

onto IKaol was found to be 114.94 mg/g. The adsorption process was pseudo-second-order, according to the kinetic experimental data. The adsorption mechanism included electrostatic attraction, H-bonding interaction, and *n-π* interaction. The adsorption results revealed that IKaol is an effective and low-cost natural adsorbent for removing cationic dyes from various types of wastewaters.

Acknowledgments
This research has been funded by Scientific Research Deanship at University of Ha'il - Saudi Arabia through project number <<RG-23 014>>. The authors would like to thank the Algerian Ministry of Higher Education and Scientific Research and General Directorate of Scientific Research and Technological Development (DGRSDT) for their support and the necessary facilities to carry out this research.

Credit author statement
Sara Bahemmi: Ideation, Methodology, Research, Analysis of Data, Visualization, Preparing, Reviewing and Editing Original Draft. **Ammar Zobeidi**: Supervision, Ideation, Methodology, Software, Research, Analysis of Data, Visualization, Preparing, Reviewing and Editing Original Draft. **Salem Atia**: Supervision assistant, Conceptualization, Investigation, Data curation. **Salah Neghmouche Nacer:** Methodology, Reviewing and Editing. **Djamel Ghernaout:** Writing review & editing. **Noureddine Elboughdiri:** Conceptualization, Writing & editing. All authors have read and agreed to the published version of the manuscript

Data availability: All data and materials are viable.
Declarations
Ethics approval and consent to participate: All authors approved**.**
Consent for publication: All authors agree to the publication.
Competing interests: The authors declare no competing interests.

References

[1] G. Z. Kyzas, J. Fu, and K. A. Matis, "The change from past to future for adsorbent materials in treatment of dyeing wastewaters," Materials, vol. 6, pp. 5131-5158, 2013.
[2] A. Mittal, J. Mittal, A. Malviya, and V. Gupta, "Removal and recovery of Chrysoidine Y from aqueous solutions by waste materials," Journal of colloid and interface science, vol. 344, pp. 497-507, 2010.
[3] M. K. Sarikulov, "Problems of Shortage of Drinking Water at the Present Stage," Web of Synergy: International Interdisciplinary Research Journal, vol. 2, pp. 873-880, 2023.
[4] C.-H. Weng and Y.-F. Pan, "Adsorption of a cationic dye (methylene blue) onto spent activated clay," Journal of Hazardous Materials, vol. 144, pp. 355-362, 2007.
[5] S. Khan, M. Naushad, M. Govarthanan, J. Iqbal, and S. M. Alfadul, "Emerging contaminants of high concern for the environment: Current trends and future research," Environmental Research, vol. 207, p. 112609, 2022.
[6] Z. Ammar, B. A. Abdelhafid, and D. Ali, "The effects of hydraulic retention time on organic loading rate in efficiency of aerated lagoons in treating rural domestic wastewater at el-oued (South-East Algeria)," Orient J Chem, vol. 33, pp. 1890-1898, 2017.
[7] A. Saravanan, S. Jeevanantham, V. A. Narayanan, P. S. Kumar, P. Yaashikaa, and C. M. Muthu, "Rhizoremediation–a promising tool for the removal of soil contaminants: a review," Journal of Environmental Chemical Engineering, vol. 8, p. 103543, 2020.
[8] D. Atia, A. A. Bebba, L. Haddad, and A. Zobeidi, "Elimination of organic pollutants from urban wastewater by illite-kaolinite local clay from south-east of Algeria," Cienc. Tecn. Vitivinic, vol. 33, pp. 17-28, 2018.
[9] S. H. Han, S. I. Kim, M.-A. Oh, and T. D. Chung, "Iontronic analog of synaptic plasticity: Hydrogel-based

ionic diode with chemical precipitation and dissolution," Proceedings of the National Academy of Sciences, vol. 120, p. e2211442120, 2023.
[10] Y.-F. Mi, G. Xu, Y.-S. Guo, B. Wu, and Q.-F. An, "Development of antifouling nanofiltration membrane with zwitterionic functionalized monomer for efficient dye/salt selective separation," Journal of Membrane Science, vol. 601, p. 117795, 2020.
[11] K. Venkatesh, G. Arthanareeswaran, A. C. Bose, and P. S. Kumar, "Hydrophilic hierarchical carbon with TiO2 nanofiber membrane for high separation efficiency of dye and oil-water emulsion," Separation and Purification Technology, vol. 241, p. 116709, 2020.
[12] S. Kumari, A. A. Khan, A. Chowdhury, A. K. Bhakta, Z. Mekhalif, and S. Hussain, "Efficient and highly selective adsorption of cationic dyes and removal of ciprofloxacin antibiotic by surface modified nickel sulfide nanomaterials: Kinetics, isotherm and adsorption mechanism," Colloids and Surfaces A: Physicochemical and Engineering Aspects, vol. 586, p. 124264, 2020.
[13] N. C. Ozdemir, Z. Bilici, E. Yabalak, N. Dizge, D. Balakrishnan, K. S. Khoo, et al., "Physico-chemical adsorption of cationic dyes using adsorbent synthesis via hydrochloric acid treatment and subcritical method from palm leaf biomass waste," Chemosphere, p. 139558, 2023.
[14] I. Khan, K. Saeed, I. Zekker, B. Zhang, A. H. Hendi, A. Ahmad, et al., "Review on methylene blue: Its properties, uses, toxicity and photodegradation," Water, vol. 14, p. 242, 2022.
[15] A. Hamidi, D. Atia, A. Rebiai, A. Reghioua, A. Zobeidi, M. Messaoudi, et al., "Investigation of adsorption kinetics and isothermal thermodynamics for optimizing methylene blue adsorption onto a modified clay with cellulose using the response surface approach," Biomass Conversion and Biorefinery, pp. 1-15, 2023.
[16] F. D. Chequer, G. R. De Oliveira, E. A. Ferraz, J. C. Cardoso, M. B. Zanoni, and D. P. De Oliveira, "Textile dyes: dyeing process and environmental impact," Eco-friendly textile dyeing and finishing, vol. 6, pp. 151-176, 2013.
[17] E. Deliyanni, E. Peleka, and K. Matis, "Removal of zinc ion from water by sorption onto iron-based nanoadsorbent," Journal of hazardous materials, vol. 141, pp. 176-184, 2007.
[18] P. Luo, Y. Zhao, B. Zhang, J. Liu, Y. Yang, and J. Liu, "Study on the adsorption of Neutral Red from aqueous solution onto halloysite nanotubes," Water research, vol. 44, pp. 1489-1497, 2010.
[19] O. A. Oyewo, O. Agboola, M. S. Onyango, P. Popoola, and M. F. Bobape, "Current methods for the remediation of acid mine drainage including continuous removal of metals from wastewater and mine dump," in Bio-geotechnologies for mine site rehabilitation, ed: Elsevier, 2018, pp. 103-114.
[20] M. Shakya, C.-C. Lo, and P. S. Chain, "Advances and challenges in metatranscriptomic analysis," Frontiers in genetics, vol. 10, p. 904, 2019.
[21] N. Cheng, B. Wang, P. Wu, X. Lee, Y. Xing, M. Chen, et al., "Adsorption of emerging contaminants from water and wastewater by modified biochar: A review," Environmental Pollution, vol. 273, p. 116448, 2021.
[22] M. K. Uddin, "A review on the adsorption of heavy metals by clay minerals, with special focus on the past decade," Chemical Engineering Journal, vol. 308, pp. 438-462, 2017.
[23] D. Atia and A. Zobeidi, "An investigation into the mineralogical and physicochemical characterization of El-Oued (Algeria) clay," Neuroquantology, vol. 20, pp. 1048-1058, 2022.
[24] P.-I. Au and Y.-K. Leong, "Surface chemistry and rheology of slurries of kaolinite and montmorillonite from different sources," KONA Powder and Particle Journal, vol. 33, pp. 17-32, 2016.
[25] E. Errais, J. Duplay, and F. Darragi, "Textile dye removal by natural clay–case study of Fouchana Tunisian clay," Environmental Technology, vol. 31, pp. 373-380, 2010.
[26] H. Ouaddari, A. Karim, B. Achiou, S. Saja, A. Aaddane, J. Bennazha, et al., "New low-cost ultrafiltration membrane made from purified natural clays for direct Red 80 dye removal," Journal of Environmental Chemical Engineering, vol. 7, p. 103268, 2019.
[27] A. Muththalib and B. A. Baudet, "Effect of heavy metal contamination on the plasticity of kaolin-bentonite clay mixtures and an illite-smectite rich natural clay," in E3S web of conferences, 2019, p. 10005.

[28] M. Shirzad-Siboni, A. Khataee, A. Hassani, and S. Karaca, "Preparation, characterization and application of a CTAB-modified nanoclay for the adsorption of an herbicide from aqueous solutions: Kinetic and equilibrium studies," Comptes Rendus Chimie, vol. 18, pp. 204-214, 2015.
[29] K. Ilaslan and F. Tornuk, "Characterization of Silver Ions-Doped Organomodified Nanoclays," Arabian Journal for Science and Engineering, vol. 48, pp. 327-340, 2023.
[30] A. Cabrera, C. Trigo, L. Cox, R. Celis, M. Hermosin, J. Cornejo, et al., "Sorption of the herbicide aminocyclopyrachlor by cation-modified clay minerals," European journal of soil science, vol. 63, pp. 694-700, 2012.
[31] N. Boutaleb, F. Chouli, A. Benyoucef, F. Z. Zeggai, and K. Bachari, "A comparative study on surfactant c etyltrimethylammoniumbromide modified clay-based poly (p-anisidine) nanocomposites: Synthesis, characterization, optical and electrochemical properties," Polymer Composites, vol. 42, pp. 1648-1658, 2021.
[32] R. Mecheri, A. Zobeidi, S. Atia, S. Neghmouche Nacer, A. A. Salih, M. Benaissa, et al., "Modeling and Optimizing the Crystal Violet Dye Adsorption on Kaolinite Mixed with Cellulose Waste Red Bean Peels: Insights into the Kinetic, Isothermal, Thermodynamic, and Mechanistic Study," Materials, vol. 16, p. 4082, 2023.
[33] B. M. Babić, S. K. Milonjić, M. Polovina, and B. Kaludierović, "Point of zero charge and intrinsic equilibrium constants of activated carbon cloth," Carbon, vol. 37, pp. 477-481, 1999.
[34] L. B. Fitaroni, T. Venâncio, F. H. Tanaka, J. C. Gimenez, J. A. Costa, and S. A. Cruz, "Organically modified sepiolite: thermal treatment and chemical and morphological properties," Applied Clay Science, vol. 179, p. 105149, 2019.
[35] L. Mouni, L. Belkhiri, J.-C. Bollinger, A. Bouzaza, A. Assadi, A. Tirri, et al., "Removal of Methylene Blue from aqueous solutions by adsorption on Kaolin: Kinetic and equilibrium studies," Applied Clay Science, vol. 153, pp. 38-45, 2018.
[36] A. H. Jawad and A. S. Abdulhameed, "Mesoporous Iraqi red kaolin clay as an efficient adsorbent for methylene blue dye: adsorption kinetic, isotherm and mechanism study," Surfaces and Interfaces, vol. 18, p. 100422, 2020.
[37] M. Kozak and H. P. Piepho, "What's normal anyway? Residual plots are more telling than significance tests when checking ANOVA assumptions," Journal of agronomy and crop science, vol. 204, pp. 86-98, 2018.
[38] N. N. Abd Malek, A. H. Jawad, K. Ismail, R. Razuan, and Z. A. ALOthman, "Fly ash modified magnetic chitosan-polyvinyl alcohol blend for reactive orange 16 dye removal: Adsorption parametric optimization," International journal of biological macromolecules, vol. 189, pp. 464-476, 2021.
[39] M. Islam and M. Mostafa, "Adsorption kinetics, isotherms and thermodynamic studies of methyl blue in textile dye effluent on natural clay adsorbent," Sustainable Water Resources Management, vol. 8, p. 52, 2022.
[40] S. Lagergren, "Zur theorie der sogenannten adsorption geloster stoffe," Kungliga svenska vetenskapsakademiens. Handlingar, vol. 24, pp. 1-39, 1898.
[41] H. Liu, R. Sun, S. Feng, D. Wang, and H. Liu, "Rapid synthesis of a silsesquioxane-based disulfide-linked polymer for selective removal of cationic dyes from aqueous solutions," Chemical Engineering Journal, vol. 359, pp. 436-445, 2019.
[42] I. Langmuir, "The adsorption of gases on plane surfaces of glass, mica and platinum," Journal of the American Chemical society, vol. 40, pp. 1361-1403, 1918.
[43] J. Appel, "Freundlich's adsorption isotherm," Surface Science, vol. 39, pp. 237-244, 1973.
[44] R. D. Johnson and F. H. Arnold, "The Temkin isotherm describes heterogeneous protein adsorption," Biochimica et Biophysica Acta (BBA)-Protein Structure and Molecular Enzymology, vol. 1247, pp. 293-297, 1995.
[45] H. J. Abdoul, M. Yi, M. Prieto, H. Yue, G. J. Ellis, J. H. Clark, et al., "Efficient adsorption of bulky reactive

dyes from water using sustainably-derived mesoporous carbons," Environmental Research, vol. 221, p. 115254, 2023.

[46] A. Oussalah and A. Boukerroui, "Removal of cationic dye using alginate–organobentonite composite beads," Euro-Mediterranean Journal for Environmental Integration, vol. 5, pp. 1-10, 2020.

[47] N. Priyantha, L. Lim, and M. Dahri, "Dragon fruit skin as a potential biosorbent for the removal of methylene blue dye from aqueous solution," International Food Research Journal, vol. 22, 2015.

[48] C. Almeida, N. Debacher, A. Downs, L. Cottet, and C. Mello, "Removal of methylene blue from colored effluents by adsorption on montmorillonite clay," Journal of colloïd and interface science, vol. 332, pp. 46-53, 2009.

[49] S. Rahmani, B. Zeynizadeh, and S. Karami, "Removal of cationic methylene blue dye using magnetic and anionic-cationic modified montmorillonite: kinetic, isotherm and thermodynamic studies," Applied Clay Science, vol. 184, p. 105391, 2020.

[50] A. Bée, L. Obeid, R. Mbolantenaina, M. Welschbillig, and D. Talbot, "Magnetic chitosan/clay beads: A magsorbent for the removal of cationic dye from water," Journal of Magnetism and Magnetic Materials, vol. 421, pp. 59-64, 2017.

[51] Y. Lv, T. Liu, J. Ma, S. Wei, and C. Gao, "Study on settlement prediction model of deep foundation pit in sand and pebble strata based on grey theory and BP neural network," Arabian Journal of Geosciences, vol. 13, pp. 1-13, 2020.

[52] A. Kausar, R. Shahzad, S. Asim, S. BiBi, J. Iqbal, N. Muhammad, et al., "Experimental and theoretical studies of Rhodamine B direct dye sorption onto clay-cellulose composite," Journal of Molecular Liquids, vol. 328, p. 115165, 2021.

[53] C. E. Onu, J. T. Nwabanne, P. E. Ohale, and C. O. Asadu, "Comparative analysis of RSM, ANN and ANFIS and the mechanistic modeling in eriochrome black-T dye adsorption using modified clay," South African Journal of Chemical Engineering, vol. 36, pp. 24-42, 2021.

[54] O. Amrhar, H. Nassali, and M. Elyoubi, "Adsorption of a cationic dye, methylene blue, onto moroccan illitic clay," J. Mater. Environ. Sci, vol. 6, p. 3054, 2015.

[55] J. Chang, J. Ma, Q. Ma, D. Zhang, N. Qiao, M. Hu, et al., "Adsorption of methylene blue onto Fe3O4/activated montmorillonite nanocomposite," Applied Clay Science, vol. 119, pp. 132-140, 2016.

[56] I. Chopra and S. B. Singh, "Kinetics and equilibrium study for adsorptive removal of cationic dye using agricultural waste-raw and modified cob husk," International Journal of Environmental Analytical Chemistry, vol. 102, pp. 7062-7083, 2022.

[57] O. L. Gaskova and M. B. Bukaty, "Sorption of different cations onto clay minerals: modelling approach with ion exchange and surface complexation," Physics and Chemistry of the Earth, Parts A/B/C, vol. 33, pp. 1050-1055, 2008.

[58] N. S. Inchaurrondo and J. Font, "Clay, zeolite and oxide minerals: natural catalytic materials for the ozonation of organic pollutants," Molecules, vol. 27, p. 2151, 2022.

[59] H. Abou Oualid, Y. Abdellaoui, M. Laabd, M. El Ouardi, Y. Brahmi, M. Iazza, et al., "Eco-efficient green seaweed codium decorticatum biosorbent for textile dyes: Characterization, mechanism, recyclability, and RSM optimization," ACS omega, vol. 5, pp. 22192-22207, 2020.